



Review article

Optimization design and performance analysis of quaternion spatial pseudo-depolarizer



Wendi Wu

School of Physics and Engineering, Qufu Normal University, Qufu, Shandong 273165, China

ARTICLE INFO

Keywords:

Depolarizer
Polarization optics
Light wave superposition
Degree of depolarization

ABSTRACT

In this study, to improve the uniformity of transmission light intensity of depolarizer, we present an optimal design of the quaternion space pseudo-depolarizer consisting of four wedge crystals. By designing the optical axis and wedge angle of each crystals, the square distribution of the output spot is realized. The mathematical expression of the degree of depolarization is obtained using the light wave superposition method. Theoretical analysis shows that the new type of depolarizer can optimize the intensity distribution of the emergent light field when the depolarizer wedge angle is sufficiently large, and it can realize the perfect depolarization of monochromatic linear polarized light. A samples of the quartz crystal material are developed and tested using lasers of 405 nm and 670 nm wavelengths. The degree of depolarization is observed to be 99% for any azimuth angle, whereas the angle of field of view is -10° – 10° .

1. Introduction

In the fields of optical measurement, communication, and space signal analysis, depolarizers are often used to eliminate the adverse effect of the polarization characteristics of light [1, 2, 3]. In the case of depolarization for monochromatic light, it generally adopts the structure of a one-element or multi-element composite with a wedge-shaped birefringent crystal, this enables the transmitted ordinary (o) and extraordinary (e) rays to produce a phase difference that varies continuously with space, so as to realize the periodic continuous change of the polarization state in space. The degree of depolarization is the average of the effect of the polarization state in space. The depolarization degree is the most important parameter for characterizing the depolarizer. The analysis of the depolarization degree is generally based on the Mueller matrix [4, 5, 6, 7, 8, 9, 10] and coherence matrix [11, 12, 13]. However, the theoretical analysis method is quite complex in the case of a depolarizer with multiple structures [14, 15]. A common type of quaternion spatial pseudo-depolarizer (dual Babinet compensator depolarizer) was analyzed in Ref. [2]. These types of depolarizers have an excellent depolarizing performance, but the intensity distribution of the transmission spot is not uniform, and it is distributed in a diamond shape.

In this study, we change the relative position of the two wedge surfaces of the spatial pseudo-depolarizer to improve the spot quality, while the transmitted spot is used for enabling equal divergence in the two orthogonal directions. This improves the uniformity of the field

distribution of the emitting spot. By using the method of superposition of polarized light waves, the depolarizing degree of a quaternion space pseudo-depolarizer with an optimized structure is analyzed, the method is simple in form, and the theoretical analysis is well-verified through experiments.

2. Structure

The Cartesian coordinate system was established, and the linearly polarized light was propagated in the positive direction along the z-axis. The structure of the new type of depolarizer is shown in Figure 1. It consists of four identical wedge crystals with wedge angle of S , wherein the wedge surfaces between parts 1 and 2 are parallel to the x-axis, and the wedge surfaces between parts 3 and 4 are parallel to the y-axis. The four-part optical axis orientation is shown in the inset of Figure 1. Within the x-o-y surface, part 1 optical axis is parallel to the y-axis, and part 2 is parallel to the x-axis. Further, part 3 is suspended at an angle of 45° to parts 1 and 2, and perpendicular to part 4.

Owing to the birefringence of the crystal, the beam-splitting phenomenon occurs when the light passes through a wedge surface (surfaces between parts 1 and 2, between parts 2 and 3, between parts 3 and 4, such as Wollaston prism). Suppose the depolarizer is made of a positive crystal, and the monochromatic polarized light is incident along the z-axis to the depolarizer; Figure 2 shows the distribution of light beam in the coordinate system (each point of light is named after the four letters

E-mail address: wuwendi@qfnu.edu.cn.

<https://doi.org/10.1016/j.heliyon.2022.e10293>

Received 1 May 2022; Received in revised form 22 June 2022; Accepted 11 August 2022

2405-8440/© 2022 The Author(s). Published by Elsevier Ltd. This is an open access article under the CC BY-NC-ND license (<http://creativecommons.org/licenses/by-nc-nd/4.0/>).

that represent different combinations of o-ray and e-ray, which in turn represent the property of the polarization states of the o-/e-rays and transformation of the four parts of the light beam in the depolarizer). Figure 2(a)–(c) exhibit the distribution of transmitted light spots when the azimuth angle (the angle between the polarization direction and y-axis) of the incident polarizing light is 0°, 90°, and arbitrary, respectively. As shown in the figure, the light spot distribution of the arbitrary angle is an exact combination of 0° and 90°. Meanwhile, the four transmitted light points have a good symmetry distributed along the four vertices of the square, and centered on the z-axis.

3. Depolarizer characteristic analysis

The incident light is considered as a plane harmonic with different propagation vectors [2, 18]. According to the symmetry of transmitted light, the angle between the transmitted beam and the x-/y-/z-axis represents the $\alpha/\beta/\gamma$ angles, respectively. The direction of propagation vectors of the light beam can be obtained from Figure 2, wherein \vec{k}_{oeoe} is $(\cos\alpha, \cos\beta, \cos\gamma)$; \vec{k}_{oeeo} is $(-\cos\alpha, \cos\beta, \cos\gamma)$; \vec{k}_{eoeo} is $(-\cos\alpha, -\cos\beta, \cos\gamma)$; and \vec{k}_{eooo} is $(\cos\alpha, -\cos\beta, \cos\gamma)$. According to the characteristics of the propagation beam vector and phase variation in the depolarizer, the initial phase difference on the surface at $z = z_0$ (an arbitrary position along the z-axis after the end-surface of the depolarizer) is

$$\varphi_{oeoe} = \frac{2\pi}{\lambda} (x \cos \alpha + y \cos \beta + z_0 \cos \gamma), \tag{1}$$

$$\varphi_{oeeo} = \frac{2\pi}{\lambda} (-x \cos \alpha + y \cos \beta + z_0 \cos \gamma), \tag{2}$$

$$\varphi_{eoeo} = \frac{2\pi}{\lambda} (-x \cos \alpha - y \cos \beta + z_0 \cos \gamma), \tag{3}$$

$$\varphi_{eooo} = \frac{2\pi}{\lambda} (x \cos \alpha - y \cos \beta + z_0 \cos \gamma), \tag{4}$$

where, λ is the wavelength of incident light.

Consider a linearly polarized light incident with an azimuth of θ and an amplitude of A , ignoring the influence of the energy loss parameters, such as absorption, reflection, and scattering of light travelling through the depolarizer. In this case, the amplitude of transmitted light would be deduced as

$$A_{eooo} = A_{eoeo} = \frac{A}{\sqrt{2}} \cos \theta, \tag{5}$$

$$A_{oeeo} = A_{oeoe} = \frac{A}{\sqrt{2}} \sin \theta, \tag{6}$$

where eooo and oeoe, eoeo, and oeoe are combined respectively, and superimposed to obtain the o-rays and e-rays (for the properties of light through the depolarizer). From Eqs. (1), (2), (3), (4), (5), and (6), the intensity and initial phase could be expressed as follows:

$$I_e = A_e^2 = \frac{A^2}{2} \left[1 + \sin 2\theta \cos \left(\frac{2\pi}{\lambda} 2y \cos \beta \right) \right],$$

$$\varphi_e = \frac{2\pi}{\lambda} (x \cos \alpha + z_0 \cos \gamma),$$

$$I_o = A_o^2 = \frac{A^2}{2} \left[1 + \sin 2\theta \cos \left(\frac{2\pi}{\lambda} 2y \cos \beta \right) \right],$$

$$\varphi_o = \frac{2\pi}{\lambda} (-x \cos \alpha + z_0 \cos \gamma).$$

Consequently, the total intensity and phase difference after superposition could be obtained as follows:

$$I = A^2 \left[1 + \sin 2\theta \cos \left(\frac{2\pi}{\lambda} 2y \cos \beta \right) \right], \tag{7}$$

$$\Delta\varphi = \varphi_e - \varphi_o = \frac{2\pi}{\lambda} 2x \cos \alpha. \tag{8}$$

The proposed design structure can be regarded as the combination of two Wollaston prisms with vertical beam splitting, and the beam splitting angle of Wollaston prisms can be obtained as [16].

$$\cos \alpha = \cos \beta = \Delta n \tan S.$$

where Δn is the birefringence of the material. Substituting into Eqs. (7) and (8),

$$I = A^2 \left[1 + \sin 2\theta \cos \left(\frac{4\pi\Delta n}{\lambda} y \tan S \right) \right], \tag{9}$$

$$\Delta\varphi = \frac{4\pi\Delta n}{\lambda} x \tan S. \tag{10}$$

From Eq. (9), it can be seen that the intensity of the transmitted light field changes periodically along the y-axis. Moreover, from Eq. (10), it can be seen that the polarization state of the transmitted light field represents the elliptical polarized light, which exhibits elliptic periodic variation along the x-axis. The depolarization principle of the depolarizer is derived from the average effect of the continuous change in space of the polarization state. The shorter the variation period, the swifter the variation and the more superior the depolarization performance [2, 16]. For a selected crystalline material, it can be seen from Eq. (9) that a larger wedge angle contributes to swifter variation. Notably, the wedge angle is the basic factor for the optimization design of depolarizer.

The elliptical polarization state of the superimposed light field is shown in Figure 3. x' and y' are the vibration directions of the transmitted e-rays and o-rays. Meanwhile, the two principal axes of the elliptically polarized light are along the x- and y-axes; a and b are their lengths, i.e., they are the amplitudes of the electric vector vibration expressions E_x and E_y on these two axes. If we suppose that the vibration directions on the x' and y' axis are E_e and E_o , respectively, the resultant equations can be expressed as

$$E_x = E_e \cos \psi + E_o \sin \psi, \tag{11}$$

$$E_y = E_e \sin \psi - E_o \cos \psi. \tag{12}$$

Then, we can obtain the following:

$$a^2 = \frac{A^2}{2} \left[1 + \sin 2\theta \cos \left(\frac{2\pi}{\lambda} 2y \cos \beta \right) \right] \left[1 + \cos \left(\frac{2\pi}{\lambda} 2x \cos \alpha \right) \right], \tag{13}$$

$$b^2 = \frac{A^2}{2} \left[1 + \sin 2\theta \cos \left(\frac{2\pi}{\lambda} 2y \cos \beta \right) \right] \left[1 - \cos \left(\frac{2\pi}{\lambda} 2x \cos \alpha \right) \right].$$

Consider

$$\Phi_x = \frac{2\pi}{\lambda} 2x \cos \alpha, \quad \Phi_y = \frac{2\pi}{\lambda} 2y \cos \beta.$$

By integrating Eqs. (10) and (11) within a period, we obtain

$$m = \int_0^{2\pi} \int_0^{2\pi} a^2 d\Phi_x d\Phi_y = 2\pi^2 A^2, \tag{14}$$

$$n = \int_0^{2\pi} \int_0^{2\pi} b^2 d\Phi_x d\Phi_y = 2\pi^2 A^2,$$

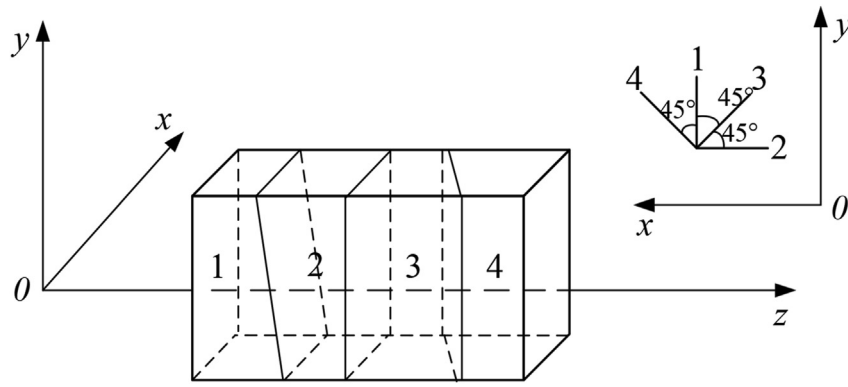


Figure 1. Structure of the new type of quaternion spatial pseudo-depolarizer.

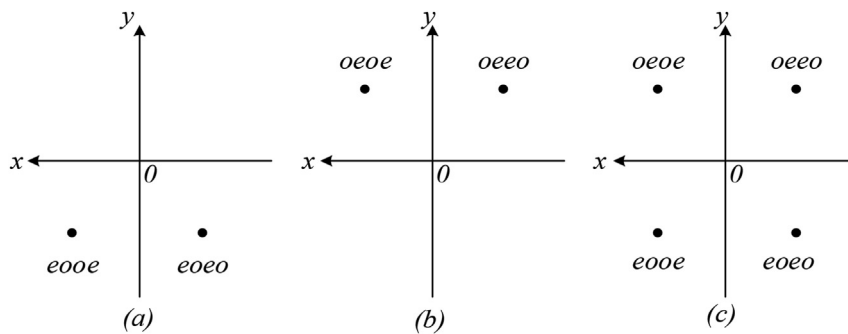


Figure 2. Distribution of transmitted light spots under incident polarized light of different azimuths: (a) 0°, (b) 90°, (c) arbitrary angle.

where m and n can be regarded as the sum of the decomposed values of the polarized light intensity of each ellipse on the two axes within a space period. Consequently, the polarization degree P of light passing through the depolarizer can be expressed as [17].

$$P = \frac{m - n}{m + n}$$

Accordingly, the degree of depolarization can be expressed as

$$D = 1 - P = \frac{2n}{m + n}$$

After substituting Eqs. (12) and (13) into Eq. (14), we obtain

$$D = 1.$$

Thus, the optimized depolarizer is observed to have a good output spot and an ideal depolarizer effect. When the wedge angle is sufficiently large, the depolarization degree could reach 100% for the linearly polarized light incident with the arbitrary wavelength and arbitrary azimuth. However, a large wedge angle will cause a greater divergence of the transmitted beam. Therefore, in the practical design of the depolarizer, the wedge angle must be designed by considering the degree of depolarizing and beam splitting. In order to avoid large beam splitting angle, we suggest that the values of α and β be designed as less than 0.1° .

4. Experimental test

A sample of quaternion spatial pseudo-depolarizer was made from four quartz crystals with a wedge angle of 6° [18], and the four parts of the depolarizer are cemented by an optical cement (model NOA61) with refractive index similar to that of quartz crystal. The complete sample thickness is 8.1 mm, and clear aperture is $12 \times 12 \text{ mm}^2$. The beam splitting angle formed by the sample is less than $1'$ [19]. The test structure is shown in Figure 4. Two laser sources were used with linearly polarized lights and wavelengths of 405 nm and 670 nm. A set of lenses

was used to shape the beam into a collimated light source with a diameter of 8 mm. By adding a corresponding wavelength of $1/4$ wave plate, the polarization state of the lasers was changed from linear polarization to circular polarization. Two Glan-Taylor (G-T) prisms were placed on a rotatable platform (to make the prism rotate on the axis of light) after the $1/4$ wave plate, and the sample was positioned between these two prisms. The azimuth of incident polarized light was changed by rotating prism G-T1 in front of the sample, and the depolarization degree of the sample was detected by prism G-T2 after rotating the sample. Finally, the transmitted light through G-T2 prism was received by the power meter (Thorlab-S121c, detector aperture is 10 mm). The sample was fixed on a five-dimensional tuner platform. The front-end of the sample was aimed toward the mid-line of the platform. The platform could be rotated

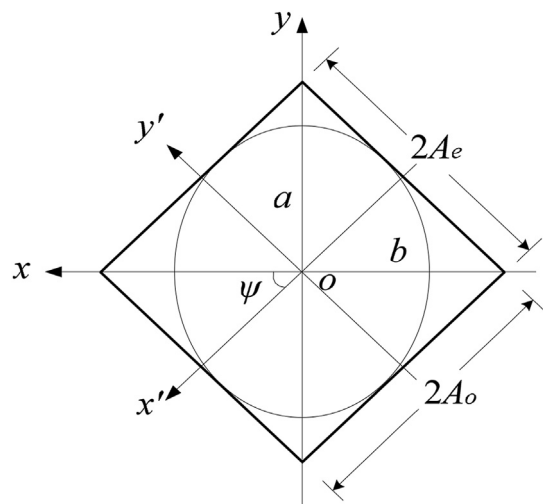


Figure 3. Elliptic polarization of the transmitted light field.

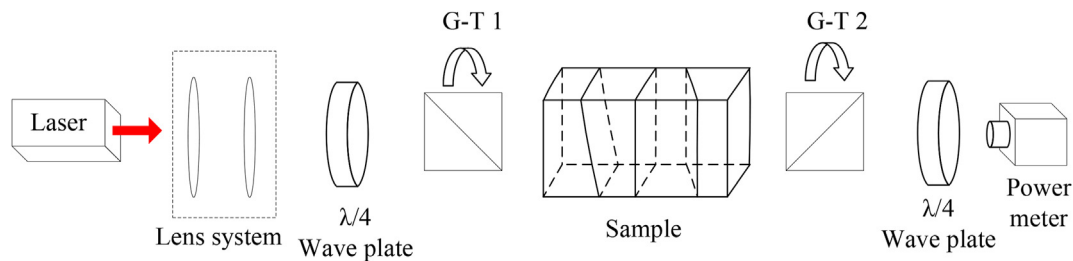


Figure 4. Test system for the degree of depolarization of the sample.

Table 1. Test results of depolarization of 405 nm light source sample.

| Rd(%) | θ (°) | | | | | | |
|---------|--------------|------|------|------|------|------|------|
| | 0 | 15 | 30 | 45 | 60 | 75 | 90 |
| i (°) | | | | | | | |
| -10 | 99.2 | 99.2 | 99.3 | 99.5 | 99.2 | 99.4 | 99.2 |
| -5 | 99.5 | 99.3 | 99.2 | 99.3 | 99.4 | 99.2 | 99.3 |
| 0 | 99.4 | 99.2 | 99.5 | 99.2 | 99.3 | 99.1 | 99.1 |
| 5 | 99.3 | 99.1 | 99.4 | 99.4 | 99.1 | 99.0 | 99.2 |
| 10 | 99.1 | 99.2 | 99.3 | 99.1 | 99.3 | 99.4 | 99.1 |

Table 2. Test results of depolarization of 670 nm light source sample.

| Rd (%) | θ (°) | | | | | | |
|---------|--------------|------|------|------|------|------|------|
| | 0 | 15 | 30 | 45 | 60 | 75 | 90 |
| i (°) | | | | | | | |
| -10 | 99.1 | 99.2 | 99.0 | 99.1 | 99.2 | 99.1 | 99.0 |
| -5 | 99.0 | 99.1 | 99.1 | 98.9 | 99.2 | 99.0 | 99.2 |
| 0 | 99.1 | 99.3 | 99.2 | 99.3 | 99.2 | 99.1 | 99.0 |
| 5 | 99.2 | 99.2 | 99.1 | 99.2 | 99.3 | 99.0 | 99.1 |
| 10 | 99.0 | 99.1 | 99.1 | 99.3 | 89.9 | 99.1 | 99.0 |

horizontally to change the incidence angle of light on the sample. The distance between the sample and the detector is approximately 0.3 m.

By adjusting the experimental light path, the light was normal incident on each component of the system. During the test, the azimuth angle was fixed first, then the degree of depolarization was tested under different incident angles. Moreover, to reduce the effect of the fluctuation of the laser power, the data were measured several times; finally, four groups of reliable data were selected.

Tables 1 and 2 show the test results of the degree of depolarization under different azimuth and incident angles for laser sources of 405 nm and 670 nm wavelengths, respectively. θ is the azimuth angle of the incident polarized light, i is angle of incidence of light, and Rd is the depolarization degree.

Notably, from the data in the table, the degree of depolarization of the new depolarizer does not change with the azimuth angle. For a depolarizer with a wedge angle of 6° , the degree of depolarization is more than 99% when the field angle is within a range of 20° . The main reason why the test results failed to reach 100% is related to the wedge angle. The theoretical analysis proved that the wedge angle is the basic factor affecting the degree of depolarization.

In addition, a $1/4$ wave plate was placed between GT-1 and the sample. The polarization state of incident light was changed by rotating the wave plate, and the depolarization degree of the sample was tested by rotating GT-2. The degree of depolarization of the sample was always higher than 98.5%, there is no obvious change as the azimuth of incident polarized light. Furthermore, the $1/4$ wave plate is moved and placed between G-T2 prism and power meter, the power of the output light does

not change significantly when the wave plate is rotated. This indicates that the output light is unpolarized.

5. Conclusion

In this paper, a new type of spatial pseudo-depolarizer with quaternary structure has been presented. The mathematical expression of the depolarization performance was obtained using the method of light wave superposition. The theoretical analysis proves that the new type of depolarizer not only optimizes the intensity distribution of the emergent light field, but also realizes the ideal depolarization of monochromatic linear polarized light sources when the wedge angle is sufficiently large. Furthermore, the depolarization degree could reach up to 100% in case of a linearly polarized light incident with an arbitrary wavelength and arbitrary azimuth. A depolarizer sample was made of quartz crystal. The sample was tested with laser sources of 405 nm and 670 nm wavelengths. The results also prove that for any azimuth and an incident angle of approximately -10° – 10° , the degree of depolarization of the sample can reach up to 99%. This design has practical significance to the signal analysis system of a large aperture in space and has been applied to several signal analysis equipment in the space field [20].

Declarations

Author contribution statement

Wendi Wu: Conceived and designed the experiments; Performed the experiments; Analyzed and interpreted the data; Contributed reagents, materials, analysis tools or data; Wrote the paper.

Funding statement

This research did not receive any specific grant from funding agencies in the public, commercial, or not-for-profit sectors.

Data availability statement

Data included in article/supp. material/referenced in article.

Declaration of interest's statement

The authors declare no conflict of interest.

Additional information

No additional information is available for this paper.

References

- [1] J. Sande, G. Piquero, C. Teijeiro, Polarization changes at Lyot depolarizer output for different types of input beams, *J. Opt. Soc. Am. A* 29 (6) (2012) 278–284.
- [2] J.P. McGuire, R.A. Chipman, Analysis of spatial pseudodepolarizers in imaging systems, *Opt. Eng.* 29 (12) (1990) 1478–1484.

- [3] T. Kubo, et al., Depolarizer improvement for optical fiber vibration sensor, in: OFS2012 22nd International Conference on Optical Fiber Sensors, Beijing, China, Proc. SPIE, 8421, 2012, 8421AK.
- [4] H.D. Noble, S.C. McClain, R.A. Chipman, Mueller matrix roots depolarization parameters, *Appl. Opt.* 51 (6) (2012) 735–744.
- [5] R. Ossikovski, O. Arteaga, Integral decomposition and polarization properties of depolarizing Mueller matrices, *Opt. Lett.* 40 (6) (2015) 954–957.
- [6] T. Grunewald, et al., Measurement of layer thicknesses with an improved optimization method for depolarizing Mueller matrices, *Meas. Sci. Technol.* 31 (11) (2020), 115010.
- [7] R. Ossikovski, Analysis of depolarizing Mueller matrices through a symmetric decomposition, *J. Opt. Soc. Am. A* 26 (5) (2009) 1109–1118.
- [8] R. Ossikovski, et al., Experimental implementation and properties of Stokes nondiagonalizable depolarizing Mueller matrices, *Opt. Lett.* 34 (7) (2009) 974–976.
- [9] N. Ortega-Quijano, et al., Experimental validation of Mueller matrix differential decomposition, *Opt Express* 20 (2) (2012) 1151–1163.
- [10] O. Arteaga, A. Canillas, Analytic inversion of the Mueller-Jones polarization matrices for homogeneous media, *Opt. Lett.* 35 (4) (2010) 559–561.
- [11] P.L. Makowski, M.Z. Szymanski, A.W. Domanski, Lyot depolarizer in terms of the theory of coherence-description for light of any spectrum, *Appl. Opt.* 51 (5) (2012) 626–634.
- [12] P. Réfrégier, M. Zerrad, C. Amra, Coherence and polarization properties in speckle of totally depolarized light scattered by totally depolarizing media, *Opt. Lett.* 37 (11) (2012) 2055–2057.
- [13] A.G. Petrashe, Depolarization of radiation upon coherent excitation, *Opt. Spectrosc.* 109 (6) (2010) 829–832.
- [14] M. Zerrad, et al., Optical systems for controlled specular depolarization, *Opt. Lett.* 39 (24) (2014) 6919–6922.
- [15] Q. Ailloud, M. Zerrad, C. Amra, Broadband loss-less optical thin-film depolarizing devices, *Opt Express* 26 (10) (2018) 13264–13288.
- [16] S.C. McClain, R.A. Chipman, L.W. Hillman, Aberrations of a horizontal-vertical depolarizer, *Appl. Opt.* 31 (13) (1992) 2326–2331.
- [17] R.A. Chipman, Depolarization index and the average degree of polarization, *Appl. Opt.* 44 (13) (2005) 2490–2495.
- [18] S.F. Ren, F.Q. Wu, W.D. Wu, Depolarization performance for monochromatic light of an improved Lyot depolarizer, *Acta Opt. Sin.* 33 (4) (2013), 0423001.
- [19] B.J. Qian, et al., Generation of vector beams using a Wollaston prism and a spatial light modulator, *Optik* 148 (2017) 312–318.
- [20] J.J. Li, et al., Polarization detection accuracy analysis of spectropolarimeter, *Infrared Laser Eng.* 47 (1) (2018), 0123002.